



National Research Institute of Astronomy and Geophysics
NRIAG Journal of Astronomy and Geophysics

www.elsevier.com/locate/nrjag



REVIEW ARTICLE

Geoelectrical exploration in the south Al Qantara Shark area for supplementary irrigation purposes – Sinai – Egypt



Mostafa Said Barseem^{*}, Talaat Ali Abd El Lateef, Hosny Mahomud Ezz El Deen, Abd Allah Al Abaseiry Abdel Rahman

Geophysical Exploration Department, Desert Research Center, 1 St. Matahaf El Matariya, El Matariya, Cairo, Egypt

Received 24 December 2014; revised 13 July 2015; accepted 10 August 2015

Available online 12 September 2015

KEYWORDS

Supplementary irrigation;
 Vertical Electrical Soundings (VESs);
 Electrical Resistivity Tomography (ERT);
 Al Qantara Shark

Abstract Sinai development is a goal of successive governments in Egypt. The present study is a geoelectrical exploration to find appropriate solutions of the problems affecting the land of a Research Station in Southeast Al Qantara. This research station is one of the Desert Research Center stations to facilitate the development of desert land for agriculture by introducing applied research. It suffers from some problems which can be summarized in the shortage of irrigation water and water logging. The appropriate solutions of these problems have been delineated by the results of 1D and 2D geoelectrical measurements. Electrical resistivity (ER) revealed the subsurface sedimentary sequences and extension of subsurface layers in the horizontal and vertical directions, especially, the water bearing layer. Additionally it helped to choose the most suitable places to drill productive wells with a good condition.

© 2015 Production and hosting by Elsevier B.V. on behalf of National Research Institute of Astronomy and Geophysics.

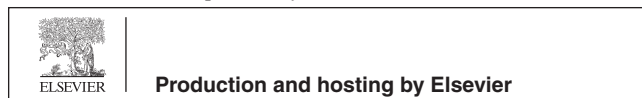
Contents

1. Introduction	164
1.1. Geomorphologic setting.	166
1.2. Geologic setting	166

^{*} Corresponding author.

E-mail addresses: barseem2002@hotmail.com (M.S. Barseem), dr.talaat41@yahoo.com (T.A.A. El Lateef), ezhosny@yahoo.com (H.M. Ezz El Deen), abaseiry@gmail.com (A.A.A.A. Abdel Rahman).

Peer review under responsibility of National Research Institute of Astronomy and Geophysics.



1.3.	Hydrogeologic setting	166
2.	Geoelectrical studies	166
2.1.	Methodology	166
2.2.	Vertical Electrical Soundings (VESs)	166
2.3.	Electrical Resistivity Tomography (ERT)	167
3.	Interpretation and results	168
3.1.	Interpretation of the vertical electrical sounding data	168
3.1.1.	Qualitative interpretation	168
3.1.2.	Quantitative interpretation	168
3.2.	Interpretation of the Electrical Resistivity Tomography (ERT) Data	170
4.	Groundwater occurrences	172
5.	Conclusions and recommendation	177
	References	178

1. Introduction

The continuous introduction of research services and scientific guidance is an important role of development. Many research stations were constructed by the Desert Research Center covering the desert land in Egypt. One of these stations is in south Al Qantara Shark that was installed in northwest Sinai for solving the agriculture problems and is also considered as a productive station. The present study concentrates on the area of this station having length reach to 1600 m and width 850 m in the northwest Sinai that covers an area equals 1360 km². It lies east of the Suez Canal between Latitudes 30°47' and 30°49'N and Longitudes 32°22' and 32°25'E and serves as a model for the adjacent areas (Fig. 1). This station suffers from a shortage of water supply needed for agriculture in some seasons, especially, the summer season, whereas it depends on one of the El Salam canal tributaries that has a shortage of water. There is one drilled well for human activity lying just south of the study area. Due to the lack of a good drainage system, some patches of water logging appear in low land at the south-west part of the area. Geoelectrical resistivity techniques are

used in the present study to deal with the previously mentioned conditions.

The geoelectrical resistivity survey techniques are used to solve many problems related to groundwater assessment, investigation, exploration and salinity. Some uses of this method in groundwater are determination of the thickness, boundaries and depths of different layers of the aquifer (Zohdy, 1989), determination of the boundary line between saline water and freshwater (El Waheidi et al., 1992; Choudhury et al., 2001), exploration of groundwater quality (Barseem, 2011; El Austa, 2000) and detection of the impact of geologic setting on the groundwater occurrence (Barseem et al., 2013). Khaled and Galal (2012) studied the impact of salt water intrusion on the groundwater occurrence. Electrical resistivity imaging surveys are widely used in many environmental and engineering studies, and also have been conducted in water covered areas (Ritz et al., 1999; Seaton and Burbey, 2000; Acworth and Dasey, 2003).

The target of this study was to solve the problems that suppressed development by carrying out geoelectrical measurements. It comprises a grid of Vertical Electrical Soundings

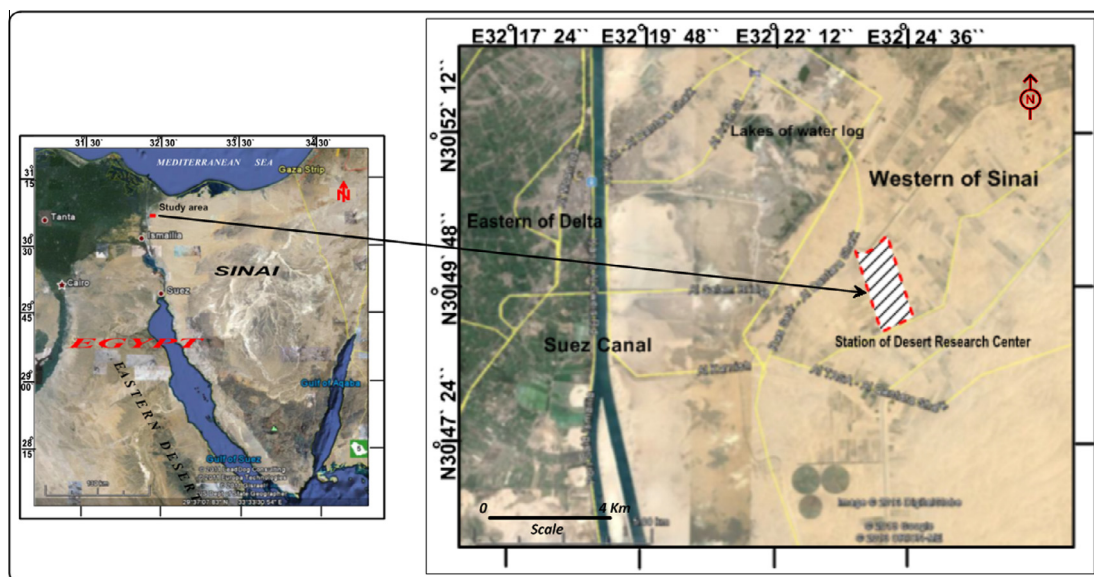


Figure 1 Location map of the Desert Research Center station at Al Qantara Shark.

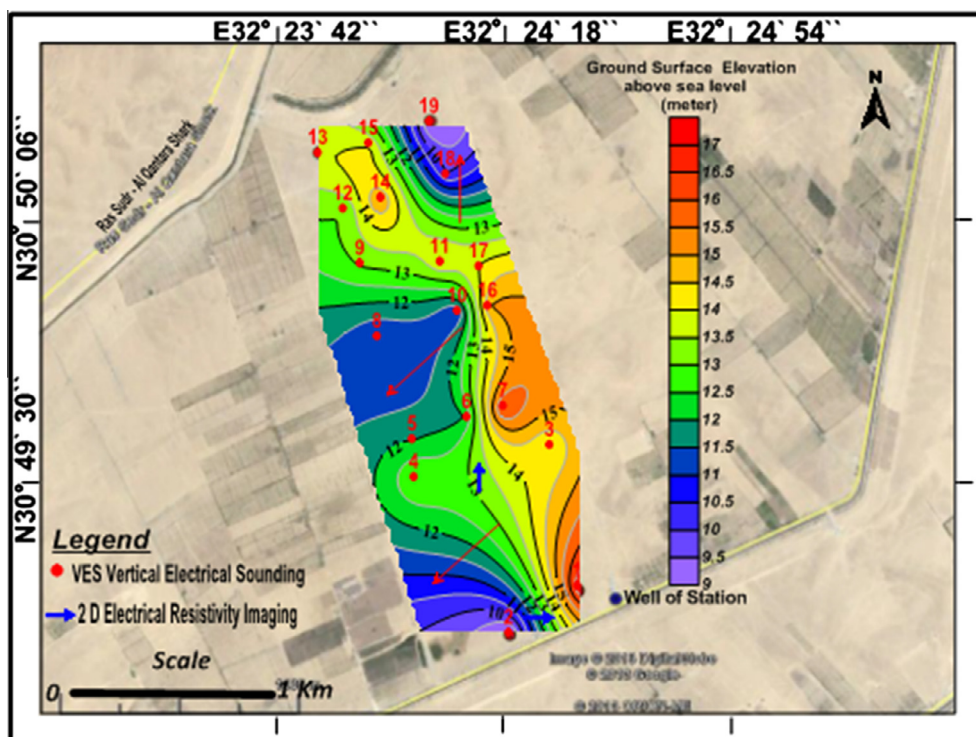


Figure 2 Contour map of the elevation values for the study area.

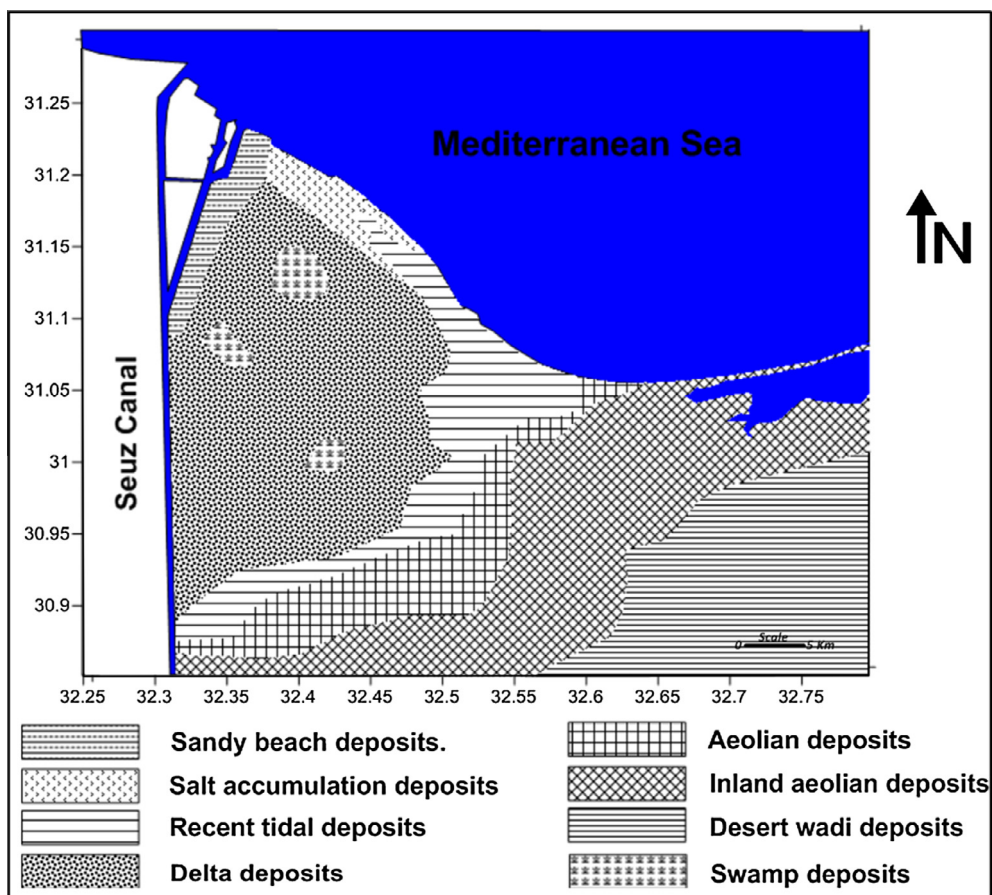


Figure 3 Geological map of the study area (After GSE, 1992 and Al Hussein et al., 2012).

(VESs) and 2-D imaging profiles covering the study area. Results can show the successive subsurface layers horizontally and vertically, and also can detect the water bearing layer, with the depth to water and its flow direction. For delineation of the lateral changes in lithological content, two dimensional imaging profiles are carried out. It can detect the different zones of water quality. Finally, the best site for drilling productive wells can be determined, as well as suitable safe discharge for the drilled wells and guide a suitable drainage system to reduce or prevent the extension of marshes.

Northwestern Sinai is located within the semi-arid belt of Egypt and is locally affected by the Mediterranean climate. This aridity is manifested by the occurrence of sand dunes and sand sheets, salt marshes and ponds as well as lack of vegetation.

1.1. Geomorphologic setting

Northwestern Sinai comprises five distinctive geomorphologic units according to [Al Hussein et al., 2012](#). It includes coastal area, El-Bardawil Lagoon, Eolian sand, Mobile sand dunes and Salt marshes and sabkhas. The study area is entirely covered by Quaternary sediments of littoral, alluvial and Eolian origin which show a variation in their texture and composition ranging from unconsolidated sands to sand and clay. [Ball, 1939](#) and [Said, 1962](#) studied the Northwestern part of Sinai that is covered by eolian sand and gravels with occasional clay interbeds of the Holocene and Pleistocene deposits. The sand dune deposits are deflected and diverted from northwest to southeast direction, most likely due to local winds. Sandy inland sabkhas are situated in low areas between hummocky surface and sand dunes. It formed as a result of high evaporation in low relief areas characterized by shallow groundwater and occasional rainfall water.

The study area is a flat to slightly undulated surface plain of eolian sand with low ground elevation which ranges from 9 m to 17 m. above sea level ([Fig. 2](#)). In the low relief area in the Southwestern direction, salt marshes and sabkhas are composed mainly of medium to coarse sands that are sometimes covered by salt crust.

1.2. Geologic setting

Northwestern Sinai is covered by Quaternary deposits of littoral, alluvial and eolian origin which show a variation in their texture and composition. These deposits range from unconsolidated sands to sand and clay ([Fig. 3](#)). The Pleistocene deposits include the Sahl El-Tineh Formation (a mixture of black and white sands with silt), the Al- Qantara Formation (sand and grits with minor clay interbeds, coquina deposits, conglomerates) and alluvial hamadah deposits ([Geological Survey of Egypt; GSE, 1992](#)). According to this map, the Holocene deposits are classified into coastal sand dunes which extend parallel to the Mediterranean Sea coast, inland sand dunes and sheets that cover large areas of northwestern Sinai (the main water bearing formation for groundwater), coastal and inland sabkhas, and interdunal playa deposits, that consist of fine sand and silt associated with evaporites ([Deiab, 1998](#)). The sand dune deposits change direction from northwest to southeast, most likely due to local winds. To the west, near the Suez Canal, northeast trending linear dunes grade progressively into

crescentic (transverse and barchans dunes) and complex crescentic dunes that are homogeneous and continuous.

1.3. Hydrogeologic setting

According to different authors such as [Said \(1962\)](#), [Shata \(1956\)](#) and [El Shamy \(1983\)](#), the Northwest of Sinai area is covered by Quaternary deposits which are composed of sand, gravel, clay and sand dunes. Either clay or sand is saturated with saline water which underlies the aquifer. The groundwater resource in the study area and its vicinity is represented by the unconfined aquifer of the Quaternary deposits. There is a drilled well in the study area with total depth of 21 m, depth to water 11 m and a maximum salinity of 2528 ppm.

2. Geoelectrical studies

Geoelectrical field work in the area of study is represented by Vertical Electrical Soundings (VESs) and Electrical Resistivity Tomography (ERT) profiles.

2.1. Methodology

The process of vertical electrical sounding takes sequential measurements of the resistance by increasing the virtual distance between the poles of the current deployment, while the center of array and the trend remains constant ([Mares, 1984](#)). The ratio between the depth of current penetration and the distance between the electrodes is called penetration factor. The depth of current penetration is of about 1/4 to 1/3 the distance between the poles of power ([Frohlich, 1974](#)). Rock resistance values are ranging from one to a few tens (ohm-m) in the mud and marl, and 10–1000 ohm-m in sand and sandstones.

Electrical Resistivity Tomography (ERT) is a useful tool to determine variations with depth in soil resistivity. The resistivity changes along the vertical and horizontal directions can be more accurate using the 2D model. The survey technique involves measuring a series of constant separation traverses.

2.2. Vertical Electrical Soundings (VESs)

The study area was covered by 19 Vertical Electrical Soundings (VESs) ([Fig. 4](#)). The Schlumberger configuration was applied in the present investigation. The current electrode separation (AB) started from 1 m and extended in successive manner to reach maximum distance 600 m. This electrode separation was found to be sufficient to reach a reasonable depth range that fulfills the aim of the study. One of these soundings (VES No. 1) was conducted beside a drilled well in order to parameterize and calibrate the geoelectrical interpretation.

The RESIST computer program ([Van Der Velpen, 1988](#)) was applied for the quantitative interpretation of the geoelectrical sounding curves. It is an interactive, graphically oriented, forward and inverse modeling program for interpreting the resistivity curves in terms of a layered earth model. An arbitrary initial model has been constructed in view of the overall shape of the sounding curves and ties to some deep drilled wells.

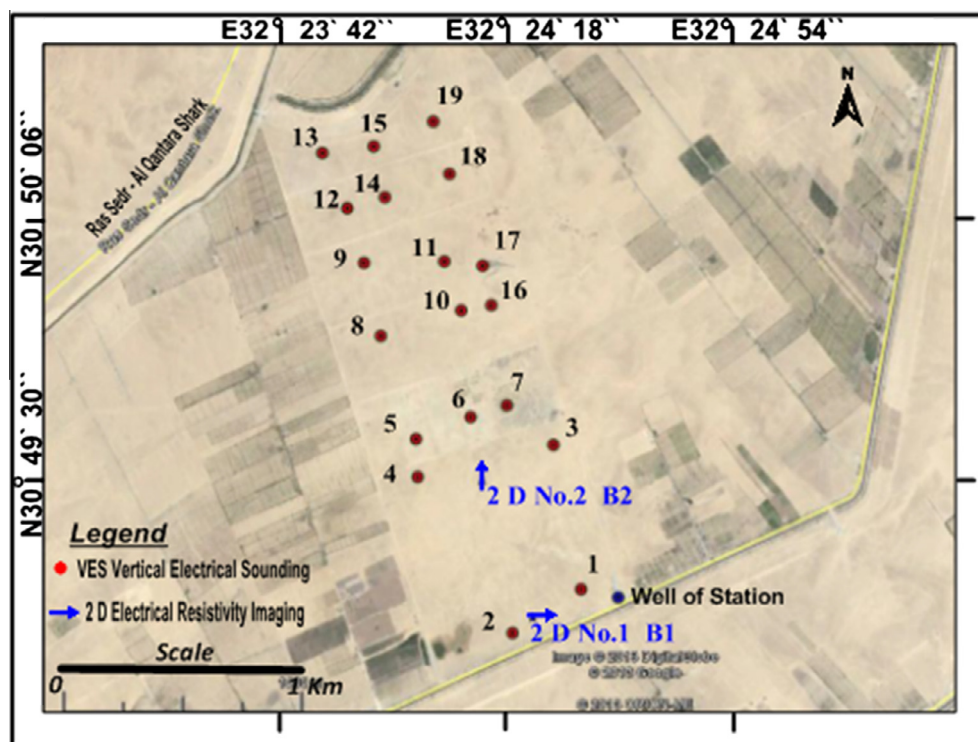


Figure 4 Location map of the Vertical Electrical Sounding (VES) and 2-D Electrical Resistivity Imaging in the study area.

Table 1 Coordinates of the measured sounding stations.

VES No.	Latitude (N.)	Longitude (E.)	Elev. (m.)	VES No.	Latitude (N.)	Longitude (E.)	Elev.(m.)
1	30°49'15.3"	32°24'30.1"	17	11	30°50'0.1"	32°24'8.3"	14
2	30°49'9.3"	32°24'19.2"	9	12	30°50'7.4"	32°23'52.8"	13
3	30°49'35"	32°24'25.7"	14	13	30°50'15"	32°23'48.8"	14
4	30°49'30.6"	32°24'4.1"	13	14	30°50' 8.9"	32°23'58.8"	15
5	30°49'35.8"	32°24'3.8"	12	15	30°50'15.9"	32°23'57"	14
6	30°49'40.4"	32°24'18.3"	12	16	30°49'54.1"	32°24'15.8"	15
7	30°49'38.8"	32°24'12.5"	16	17	30°49'59.5"	32°24'14.1"	14
8	30°49'49.9"	32°23'58.2"	11	18	30°50'15.3"	32°24'9.1"	10
9	30°49'59.9"	32°23'55.5"	13	19	30°50'19.3"	32°24'6.5"	9
10	30°49'53.4"	32°24'11"	11				

2.3. Electrical Resistivity Tomography (ERT)

Two imaging profiles are conducted (Fig. 4) to verify the results of Vertical Electrical Sounding (VES) especially, the boundary between geoelectrical layers. One of these imaging profiles was measured from west to east and other from south to north. The resistivity changes along the vertical and horizontal directions can be more accurate using the 2D model. The survey technique involves measuring a series of constant separation traverses. In the present study, the Wenner electrode array is applied where the measurements start at the first traverse with a unit electrode separation “a” equals 5 m and increase at each traverse by one unit i.e. 10, 15, 20, ..., n to reach 105 m.

For the interpretation of the imaging data, the computer program RES2DINV, ver 3.4 written by [Loke \(1998\)](#) was used. It is a Windows based computer program that automatically determines a two-dimensional (2-D) subsurface resistivity

model for data obtained from electrical imaging surveys ([Griffiths and Barker, 1993](#)).

The direct current resistivity meter “Terrameter” model SAS 1000 C was used for measuring the resistance “ R ” with 0.5% precision. The locations (latitudes and longitudes) of the sites of the geoelectrical measurements and their elevations relative to sea level were determined using the geographic positioning system (GPS) apparatus (Trimble type) in contact with nine satellites, and topographic maps of scale 1:50,000. The obtained locations and ground elevations are listed in [Table 1](#).

The interpretation of the geoelectrical resistivity data depends on determining and verifying the geoelectrical parameters i.e. resistivities and thicknesses, of a series of layers. The interpretation includes also correlation of similar layers where a layer or some layers may be absent because of lithologic variations. The results are a geological model that can be reflected in terms of lithological variation and stratigraphy.

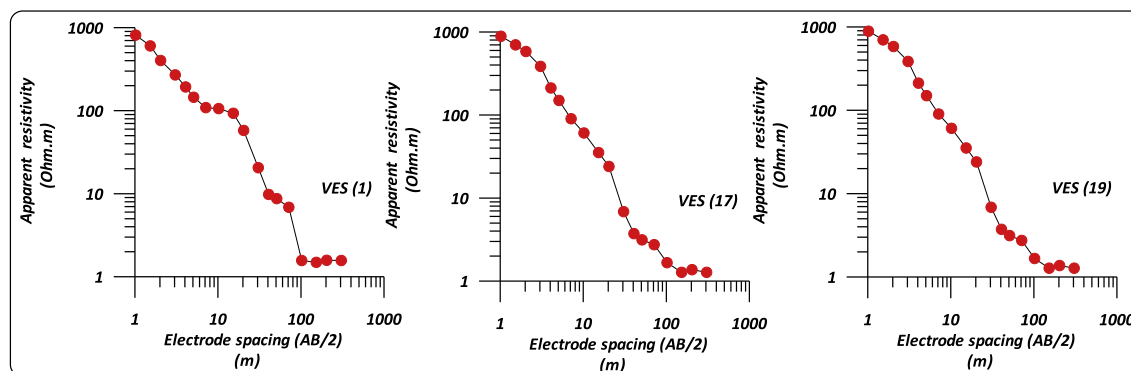


Figure 5 Examples of the resistivity sounding curves.

3. Interpretation and results

The interpretation of Vertical Electrical Sounding (VES) data comprises qualitative and quantitative processes. The qualitative interpretation includes a comparison of the relative changes in the apparent resistivity and thickness of the different layers. It gives information about the number of layers and their continuity throughout the area or in a certain direction and reflects the degree of homogeneity or heterogeneity of the individual layer. The quantitative interpretation, on the other hand, involves the determination of the number of the geoelectrical layers as well as the “true” or interpreted depth, thickness and resistivity of each layer.

The computer program automatically determines a two-dimensional (2-D) resistivity model for the subsurface using the data obtained from the imaging survey. The results of interpreting geoelectrical field data are shown in the following sections.

3.1. Interpretation of the vertical electrical sounding data

The delineation of the subsurface sequence of the geoelectrical layers according to the qualitative and quantitative interpretation is as follows.

3.1.1. Qualitative interpretation

A preliminary qualitative interpretation of the sounding curves using partial curve matching (Orellana and Mooney, 1966) provides the initial estimates of the resistivities and thicknesses (layer parameters) of the various geoelectrical layers. The qualitative interpretation of the field curves (Fig. 5) indicates generally, QQ types of the vertical electrical sounding curves, exhibiting homogeneity in resistivity values. It shows a decrease in resistivity values with depth due to increases clay content and salinity with depth, while high resistivity values reflect sand deposits. Generally, homogeneity in thickness can be detected from the curves but there is a variation in the last cycle on curves of VES's No 17 & 19 in the north-western part of the area.

3.1.2. Quantitative interpretation

The quantitative interpretation involves the determination of the number of the geoelectrical layers as well as the true depth, thickness and resistivity of each layer. The geologic setting and relevant information are visualized and described in view of a number of generated geoelectrical cross sections crossing the concerned site in different directions, and finally by the construction of contour maps. Fig. 6 shows the interpretation of

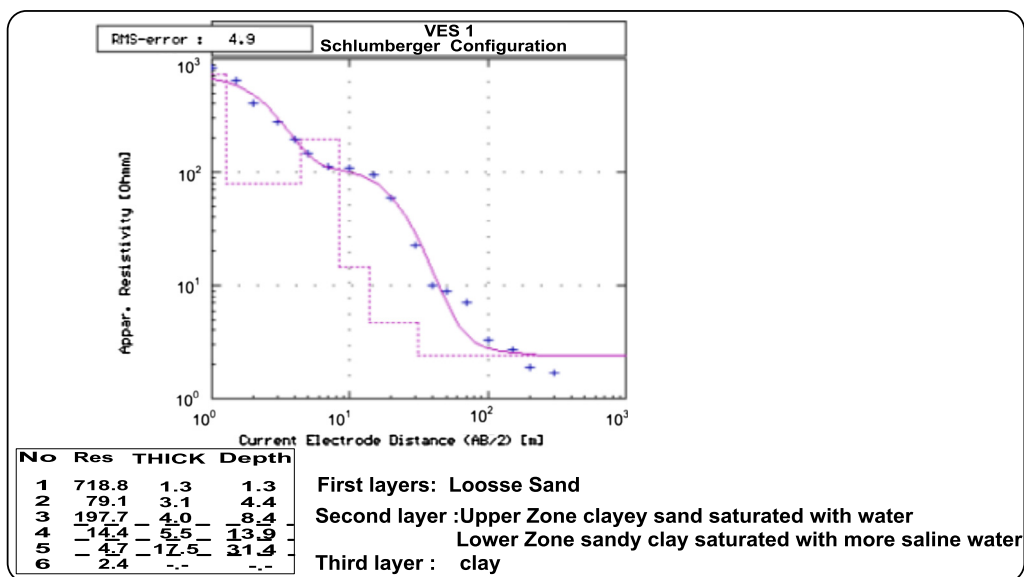


Figure 6 The S-N geoelectrical cross section AA'.

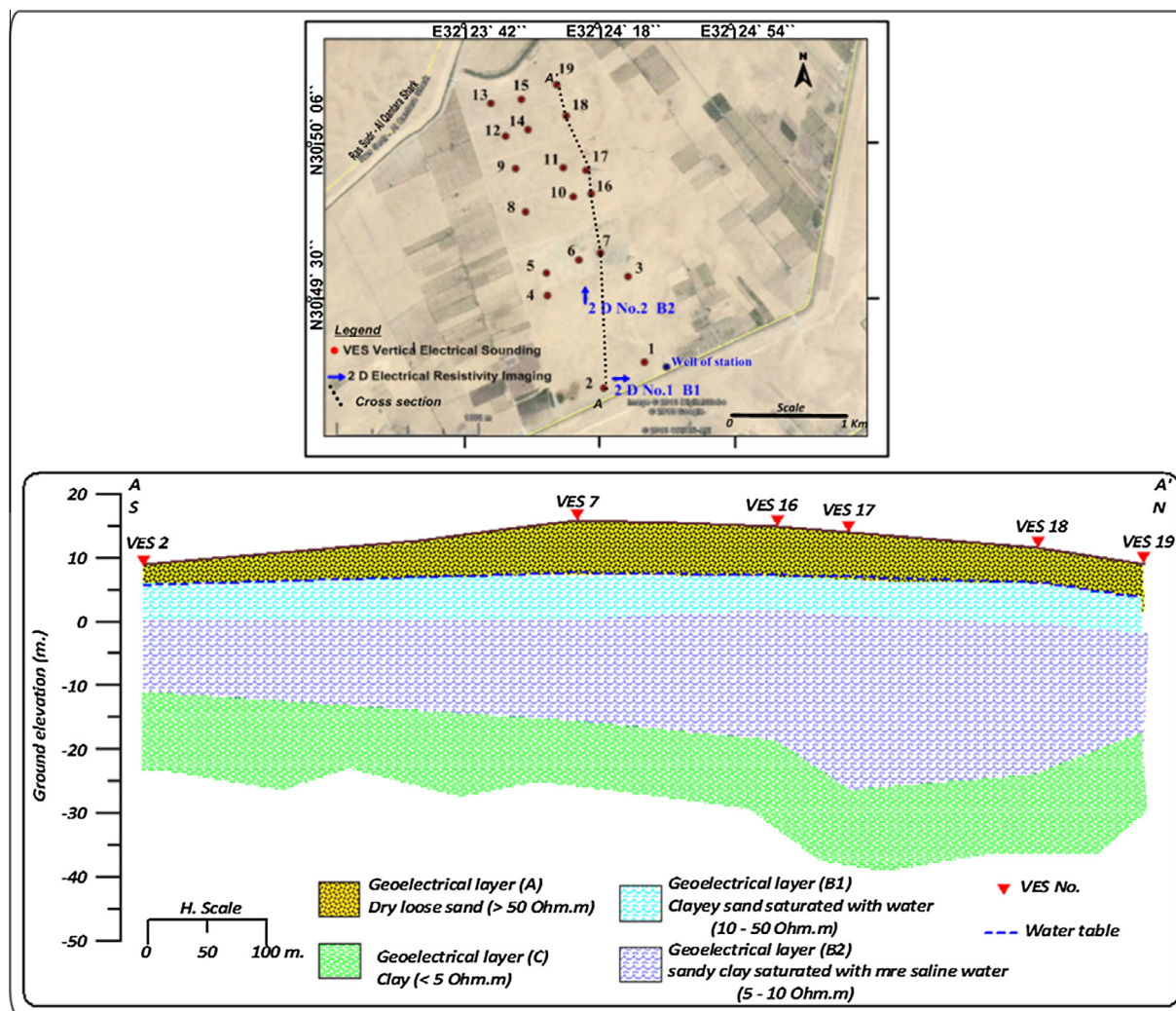


Figure 7 The geoelectrical results and lithologic data at VES No. 1, located near the drilled well.

the modeled resistivity sounding VES No. 1, located beside a drilled well. The results of the geoelectrical interpretation (Table 2) are correlated with available lithological information obtained from a well that was found in the study area. Three geoelectrical layers can be detected and their parameters (resistivity and thickness) are listed in Table 3.

The detailed interpretation results of the geoelectrical resistivity sounding measurements in the study area are discussed as follows.

3.1.2.1. The subsurface geoelectrical succession. The geoelectrical succession is formed of a number of layers being grouped together in three main layers. In order to make the abovementioned description more illustrative the geoelectrical parameters of the interpreted layers are determined. The first layer is surface layer “A”. The second is layer “B”, divided according to resistivity values into two zones (B1 and B2). The last one is layer “C”. A description of each of these geoelectrical layers is as follows:

- Layer “A”

The surface layer (A) consists of three thin dry layers grouped in one layer to reach optimum correlation between

the geoelectrical layers and the predominant geologic units. The resistivity of such a layer is plausibly expressed in terms of the average transverse resistance (ρ_t or T). This parameter can be calculated from the resistivities and thicknesses of the group of thin layers as follows:

$$\rho_t = \sum (\rho_i \cdot h_i) / \sum h_i \dots i = 1 \text{ to } n;$$

where ρ_i is the resistivity of the i th layer, h_i is its thickness and n is the number of layers. This layer is formed from sand and clay content with resistivity larger than 50 Ohm-m and whose thickness does not exceed 12 m.

- Layer “B”

The second layer (B) consists of two zones (B1 and B2) according to resistivity values and is probably formed of saturated sand. The upper zone (B1) exhibited resistivity less than 50 Ohm-m and maximum thickness of 5 m, while the lower zone (B2) showed resistivity ranges from 5 to 10 Ohm-m and thickness varying from 15 to 30 m. The changes in resistivity values reflect the degree of dissolved solids in the groundwater, so the lower zone (B2) is more saline than the upper one (B1). The resistivity values decrease downward with depth until reaching the last layer. This water bearing layer (B) can be

Table 2 Resistivities and corresponding thicknesses at Vertical Electrical Sounding stations.

VES No.	Goelectrical layer (A) (Dry loose sand)						Goelectrical layer (B)				Goelectrical layer (C)	
							Upper zone (B1)		Upper zone (B2)			
	ρ_1	h_1	ρ_2	h_2	ρ_3	h_3	ρ_4	h_4	ρ_5	h_5	ρ_6	h_6
1	718.8	1.3	79.1	3.1	197.7	4.0	14.4	5.5	4.7	17.5	2.4	–
2	600.2	1.0	57.5	1.7	168.0	0.7	13.0	5.5	4.1	16.3	0.7	–
3	736.7	0.4	252.8	2.3	137.8	5.9	37.7	6.2	4.1	16.6	1.2	–
4	156.6	3.2	11.2	1.5	92.8	3.4	17.6	5.5	8.6	18.8	1.4	–
5	595.9	0.6	217.2	2.1	118.5	2.4	18.2	5.2	7.6	19.6	1.6	–
6	656	0.9	367.5	1.1	213.1	5.1	23.9	5.6	6.0	14.1	1.3	–
7	1200.3	0.4	431.9	1.7	108.7	6.2	20.6	7.2	9.3	16.4	1.6	–
8	1999.6	0.4	146.9	1.6	80.5	3.0	19.0	5.3	6.8	18.6	1.4	–
9	1864.5	0.5	317.1	0.9	89.6	4.8	17.3	5.0	3.8	18.8	1.3	–
10	876.5	0.5	382.6	1.5	133.3	3.0	32	4.8	5.1	14.3	1.7	–
11	2607.7	0.4	215.9	1.4	84.3	5.5	13.7	5.8	7.9	22.0	2.3	–
12	1169.9	0.4	223.6	1.2	141.2	3.4	31.8	4.8	8.4	18.6	2.1	–
13	803.5	0.6	91.4	1.1	118.8	6.4	37.0	5.4	9.8	29.0	1.8	–
14	817.6	0.7	116.6	1.0	162.1	5.9	37.5	5.5	7.6	18.1	2.0	–
15	1407.8	0.3	408.0	1.9	159.2	6.2	33.7	5.3	6.2	16.5	1.4	–
16	1300.9	0.6	449.3	1.0	133.0	6.0	31.0	5.2	8.2	21.0	1.5	–
17	2015.6	0.4	246.0	0.4	90.4	7.5	30.0	4.9	7.7	27.0	0.8	–
18	3648.3	0.3	188.1	1.4	87.7	4.8	28.7	5.1	7.7	22.0	0.9	–
19	1022.2	0.7	670.6	0.7	103.1	4.0	34.5	4.7	6.7	16.5	1.3	–

Table 3 Resistivities and the thicknesses range and the corresponding lithologic composition of the detected goelectrical layers.

Layer No.	Resistivity (Ohm m)	Thickness (m)	Corresponding lithology
Goelectrical layer (A)	> 50	1–5	Dry loose sand
Goelectrical layer (B)	Upper zone (B1)	10–50	Clayey sand saturated with water
	Lower zone (B2)	5–10	Sandy clay saturated with more saline water
Goelectrical layer (C)	< 5	Clay

called a perched aquifer due to the presence of lower impermeable clay layer.

• Layer “C”

The last detected layer (C) consists of clay with resistivity value less than 5 Ohm-m. It acts as a barrier that prevents vertical groundwater passage.

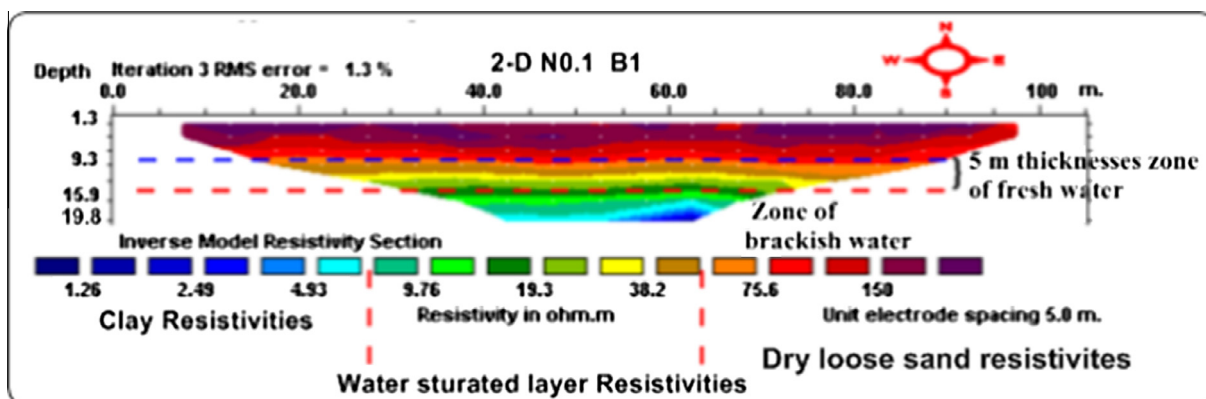
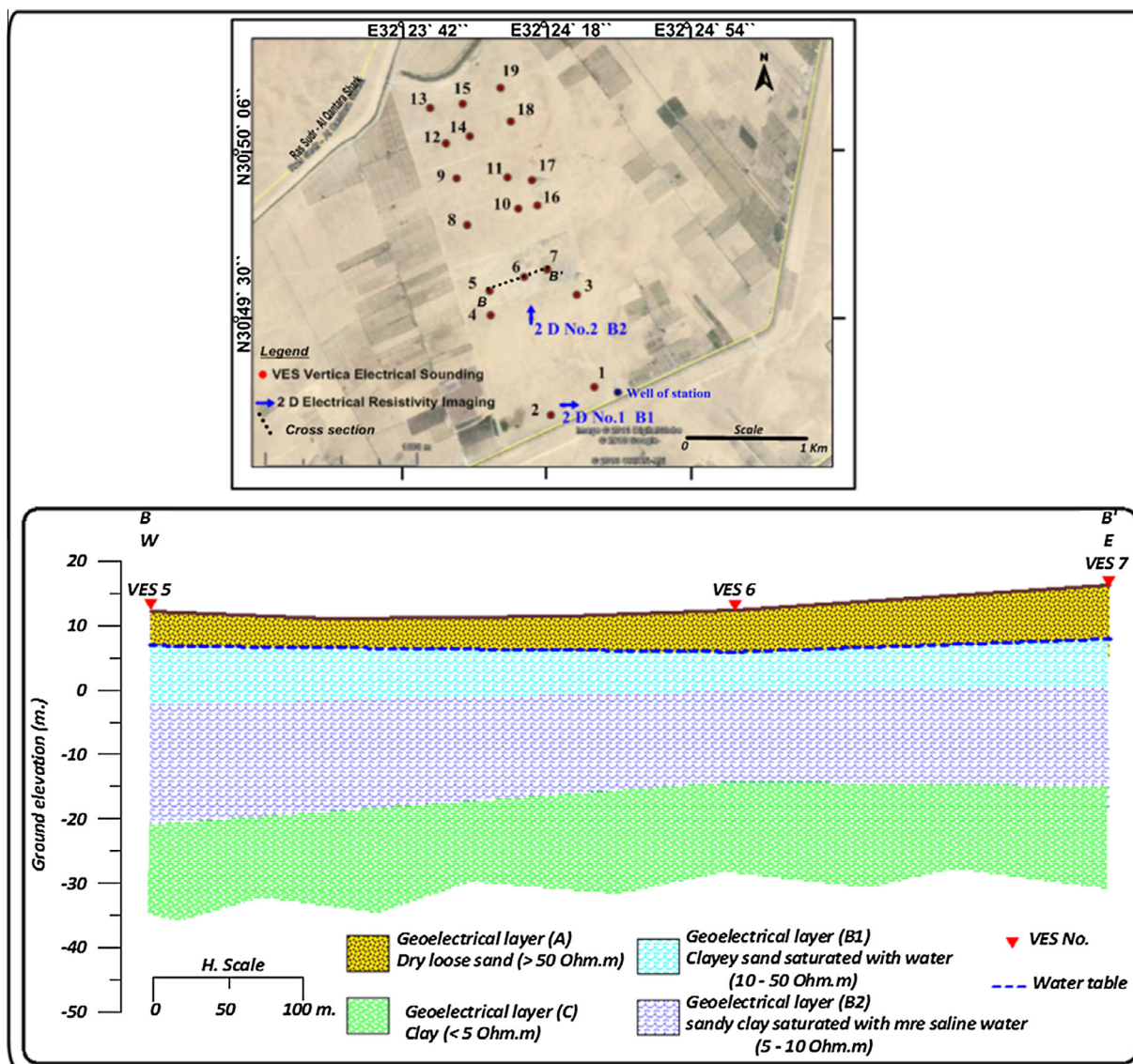
3.1.2.2. The goelectrical cross sections. These sections illustrate the goelectrical sequence, and lateral and vertical variation for different layers along the profile direction. Two goelectrical cross sections are constructed: one section has south–north direction (Fig. 7), while the other section has west–east direction (Fig. 8). The detailed description of the goelectrical layers from top to bottom can be described as follows:

1. Generally, the goelectrical cross sections (A-A') and (B-B') (Figs 7 and 8) consist of three goelectrical layers “A”, “B”, and “C”. The surface layer (A) is formed of sand deposits, and the second layer (B) is divided into two zones (B1 and B2) acting as water bearing units. It is formed dominantly of sand and the last layer (C) consists of clay.
2. These layers exhibited a regular thickness except for a change in the relief of the last clay layer at VES's No. 17 & 19 in the NE corner of the study area due to lateral lithological changes.

3. The resistivity values of the goelectrical layers decrease downwards in the study area due to increasing clay content and increasing salinity.
4. The first goelectrical layers decrease in thicknesses in the southwards.
5. The thickness of the saturated water bearing layer (B) generally increases toward the southeast direction.
6. The groundwater is shallower toward the south due to lower surface elevation but it becomes deeper at VES's No. 6, 16 & 17 in the center of the study area.

3.2. Interpretation of the Electrical Resistivity Tomography (ERT) Data

The interpretation results of the 2D goelectrical measurements show horizontal and vertical changes in goelectrical resistivity and thickness of the layers. Examination of the imaging profiles at the two selected sites (B1 and B2) in the study area (Figs. 9 and 10) indicates that zones of high resistivity correspond to the dry coarse-grained sand that dominates the upper parts. These images show an obvious downward resistivity decrease that represents saturated sand deposits. Two goelectrical layers can be detected. The upper layer is the surface layer of the study area with high resistivity values reflecting homogeneous dry sand. The lower layer is saturated with water and is divided into two zones according to resistivity differentiation. The first zone exhibited resistivity values



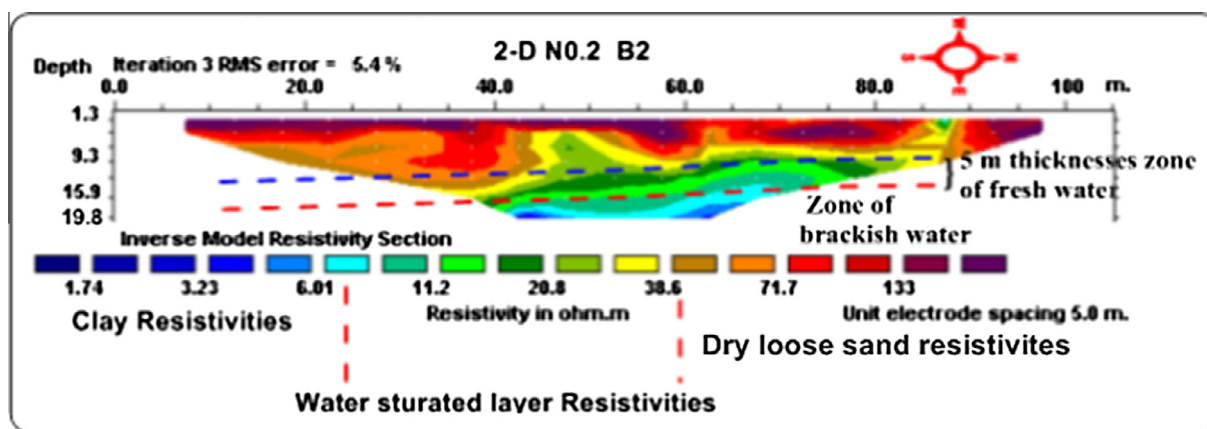


Figure 10 Inversion result of 2-D resistivity imaging profile at site B2.

ranging from 10 to 50 Ohm-m, relatively higher than the second zone which exhibited resistivity values less than 10 Ohm-m. This means that the lower zone is more saline than the upper one.

The depth to water reaches 8 m from the ground surface. The thickness of the upper zone is 5 m and is composed of sand and clayey sand. The base of the lower zone was not detected but is composed of sandy clay and clay. These results are compatible with the interpretations of Vertical Electrical Soundings (VESs).

4. Groundwater occurrences

According to the limited hydrogeological information in the study area, the applied geoelectrical methods were integrated to collect the common features that may suggest groundwater occurrence. The Quaternary aquifer consisting of sand and gravel (unconfined aquifer) dominates the area of study. There is one drilled well in the area of study with total depth of 21 m and depth to water of 11 m. Its salinity was measured as 2528 ppm. As mentioned above, the study area belongs to a research station for agriculture and depends on the tributary of the El Salam Canal for irrigation. The problem in this area is the deficiency of irrigation water. Thus, the results of the geoelectrical measurements were applied to this problem to suggest a suitable solution.

The interpretation of geoelectrical data of both the Vertical Electrical Soundings and 2D imaging reveals that the second layer (B) acts as a water bearing layer. It is divided into two zones (B1 and B2) according to resistivity values that reflect the degree of salinity, wherein the lower one is more saline than the upper. The isoresistivity contour maps (Figs. 11 and 12) of the two saturated zones (B1 and B2) are constructed for more details. Layer B1 showed increased resistivity toward the northeastern direction. Layer B2 exhibited high resistivity values in the northeastern and southwestern directions. This means that the priority sites recommended for wells to be drilled can be chosen in these trends. Generally, the upper saturated zone has better groundwater quality than the lower saturated zone, as the resistivity values of the upper zone are higher than the lower ones. For more detail about the quality of the water bearing layer (B), both resistivity and thickness values (B1 and B2) are combined in terms of the average transverse resistance

(Table. 2). The constructed contour map (Fig. 13) for these results shows a generally, an increase in groundwater quality toward the north and east directions.

The thickness of saturated layer “B” is an important geoelectrical parameter for judging suitable sites for drilling future wells. The isopach contour maps (Figs. 14 and 15) for B1 and B2 were constructed. They show an increase in thickness values in the northeastern and southwestern directions, and generally the lower saturated zone (B2) has greater thickness than the upper saturated zone (B1).

The level of the water bearing layer related to sea level from the VES results is used to construct a contour map (Fig. 16) of the water table elevation. It shows the groundwater flow direction. The level contour map clarifies the groundwater flow in two directions. The first flow direction is toward the southwestern trend of the study area. This is caused by accumulation of groundwater in this site that appears as a pond in the area related to a raise of the clay layer. The second flow direction is toward the northeastern trend where the depth to the clay layer has a large value in this location. It is obvious that the clay layer played an important role in the groundwater configuration; hence, a contour map (Fig. 17) of the depth of the clay layer was also constructed. This map shows a generally, an increase in depth of the clay layer toward the northeastern direction. According to this information, the most suitable place for a drainage system is in the southwestern direction where there is less depth to the clay.

The geoelectrical results locate the best priority sites for drilling productive wells for supplementary irrigation in the study area in the northeastern and southeastern directions. These wells must be drilled with total depth not exceeding 30 m. The suitable technique for drilling is hand dug but possible use of a rotary drill would be to detect depth. Proper construction practices must be observed for drilled wells to construct a suitable casing. Also, pumping tests are important for determining safe yield and serve to indicate areas of good quality of groundwater recharge.

Because of the small thickness of the upper saturated zone (B1) of approximately 5 m. of good quality groundwater, it is here suggested to construct three cement storage basins with dimensions of 3 * 20 * 20 m. These basins will permit collecting a water volume of approximately 1200 m³. This collected water can be used during shortages of water in the tributary of the El Salam canal. The distribution of these basins may be as

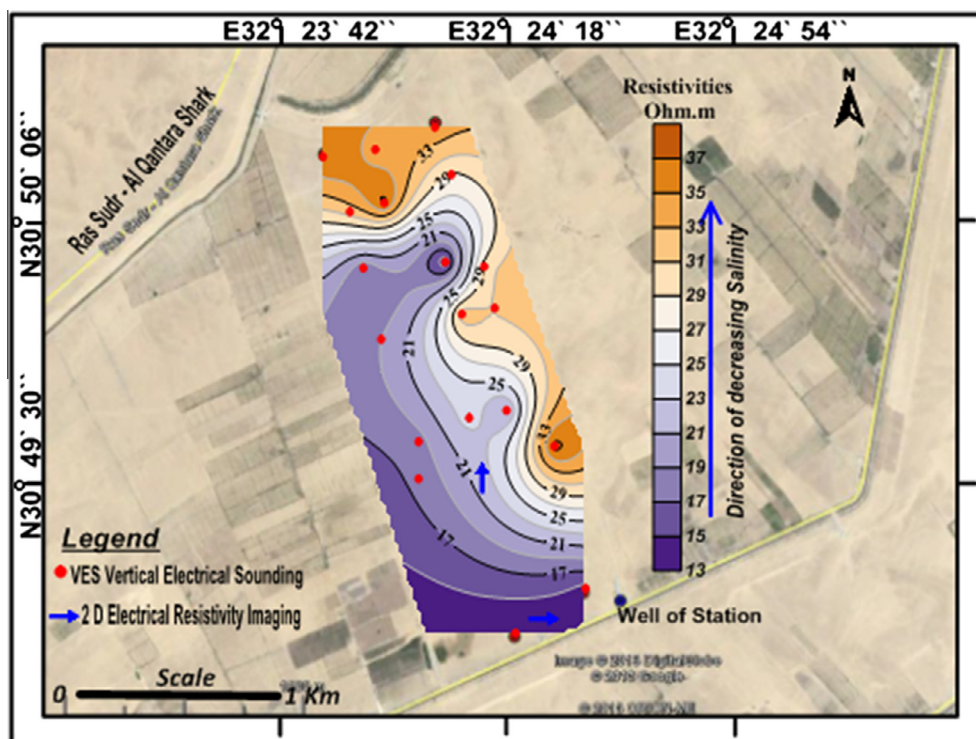


Figure 11 Isoresistivity contour map of upper saturated zone B1.

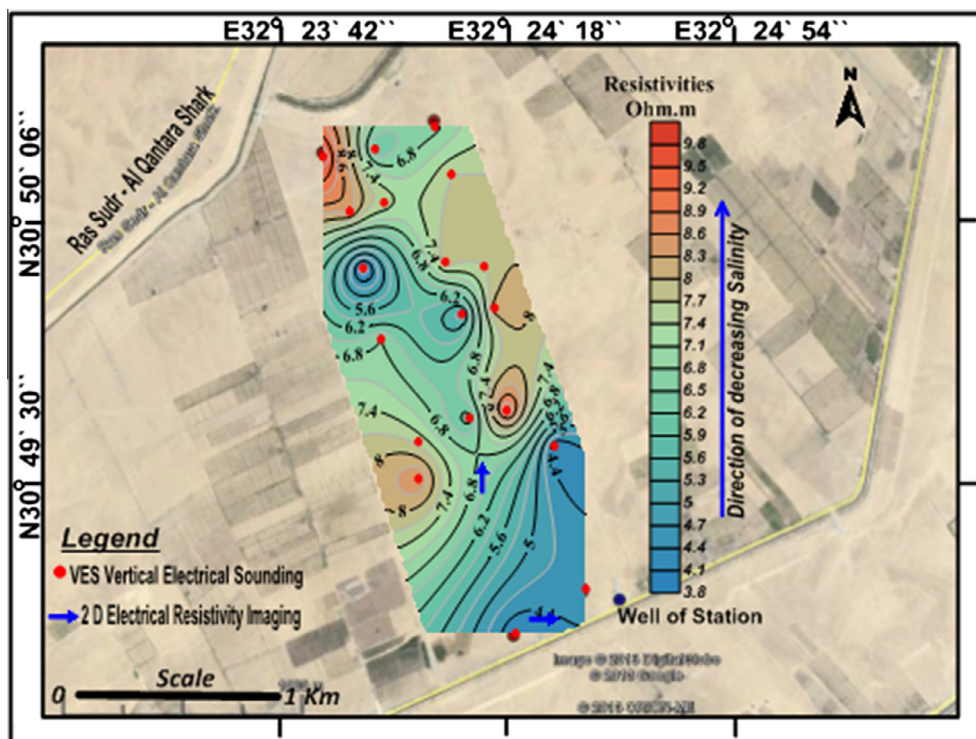


Figure 12 Isoresistivity contour map of lower saturated zone B2.

follows: one constructed in SW corner of the study area using the existing water in the ponds for recharge, and the other two basins should be constructed in the center and the N end of the study area as shown in Fig. 18.

Geoelectrical measurements indicate two saturated zones (B1 and B2) with different salinities. The upper saturated zone (B1) is in good quality groundwater and lower salinity than the lower saturated zone (B2). So, precautions must

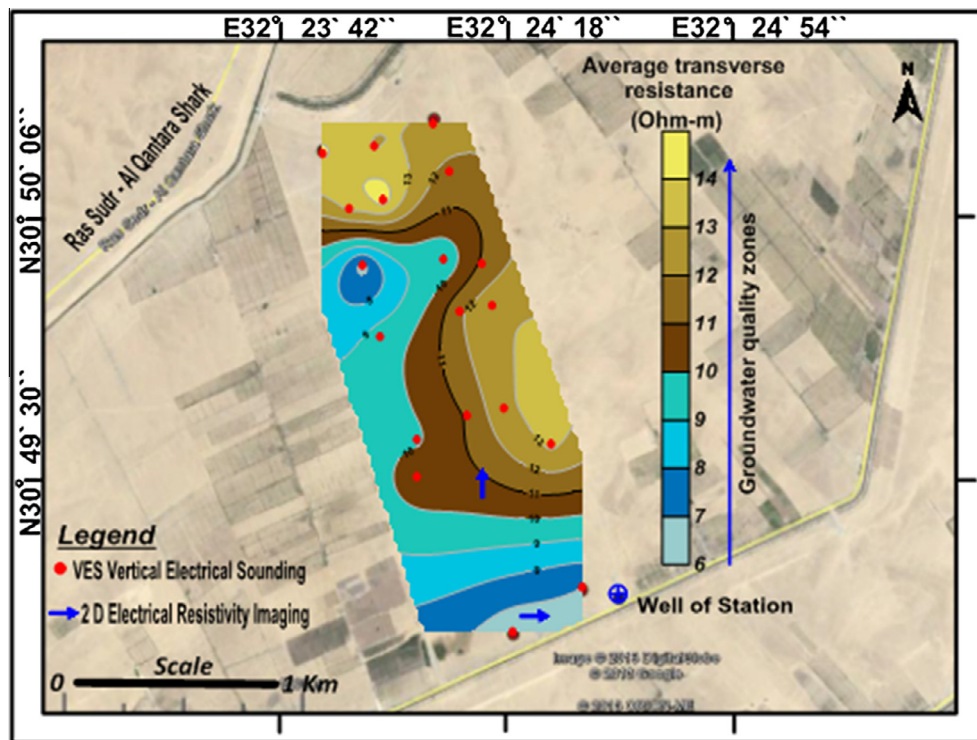


Figure 13 Average transverse resistance contour map of layer B.

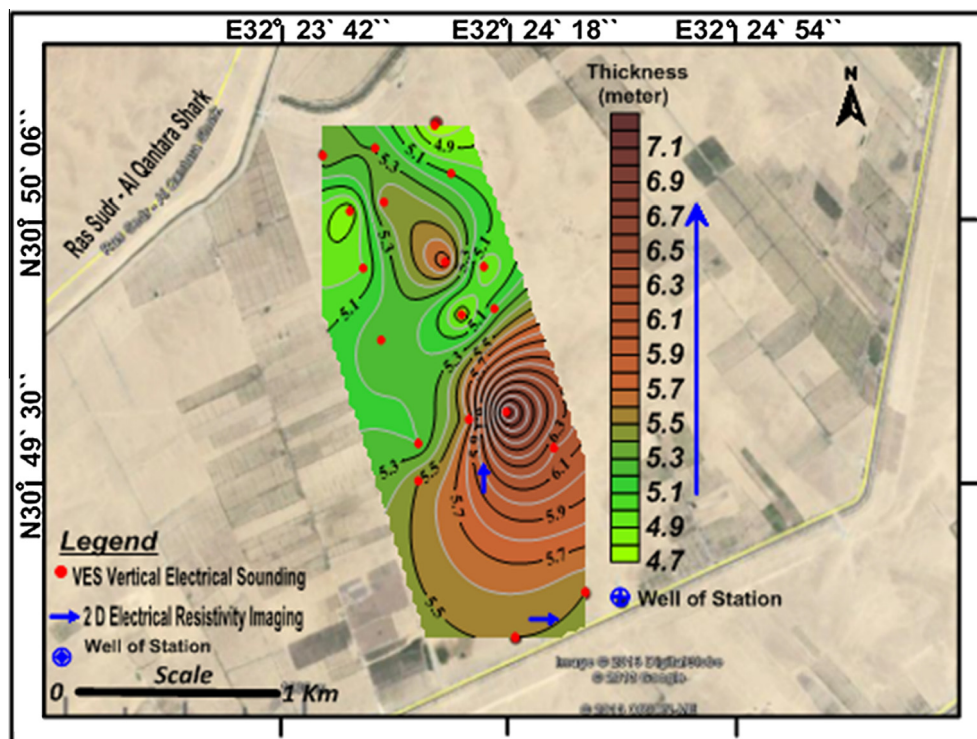


Figure 14 Isopach contour map of upper saturated zone (B1).

be made to never exceed the safe yield for preventing a mixing of the groundwater of both saturated zones (B1 and B2) during discharge from wells and consequence harmful effect on cultivation. When an aquifer contains

an underlying layer of saline water such as in this study area and is pumped by a well penetrating only the brackish water of the upper part of the aquifer, a local rise of the interface between the saline and brackish water

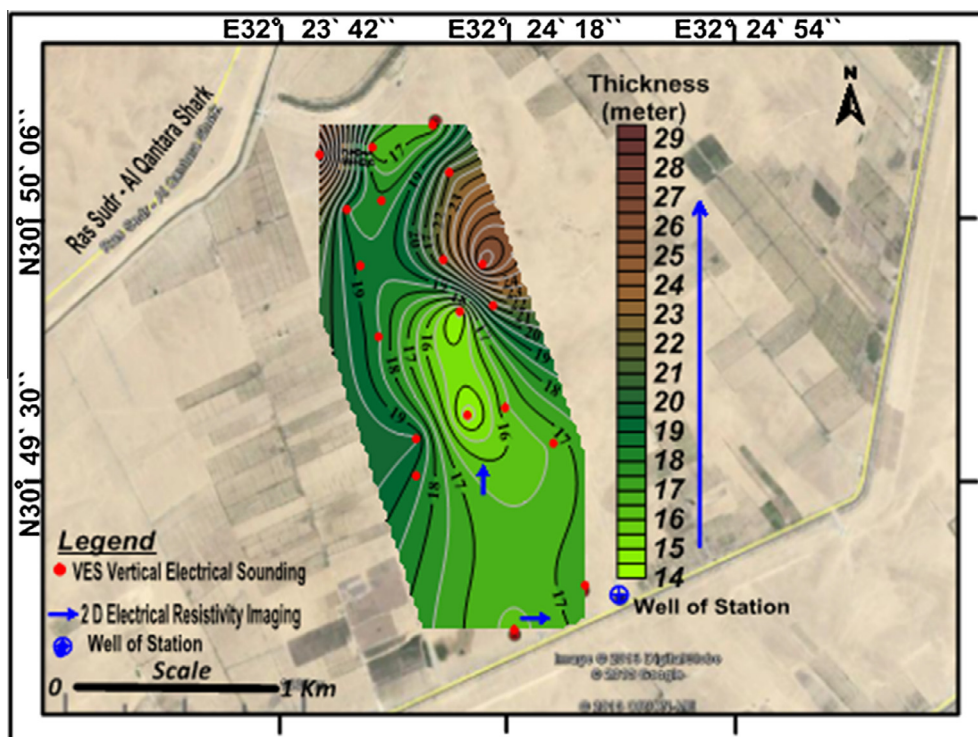


Figure 15 Isopach contour map of lower saturated zone (B2).

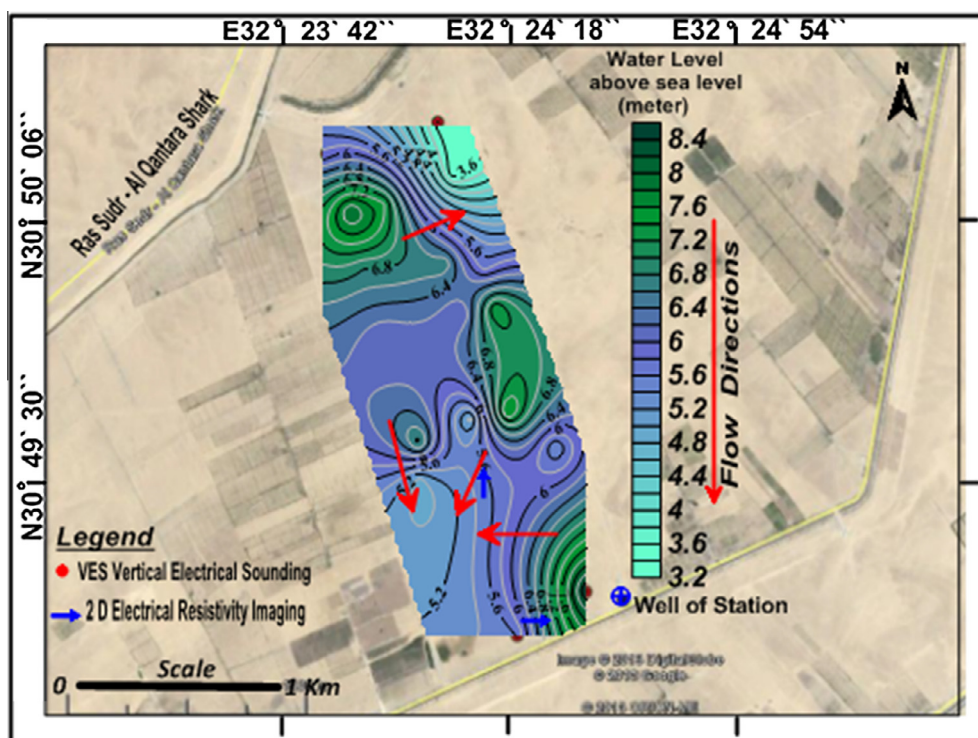


Figure 16 Water table contour map.

below the well occurs. This phenomenon is known as up-coning, by pumping. This generally necessitates that the well has to be shut down because of the influence of the saline water. Up-coning is a complex phenomenon

and only in recent years has significant headway been made in research to enable criteria to be formulated for the design and operation of wells for skimming brackish water from above the saline water.

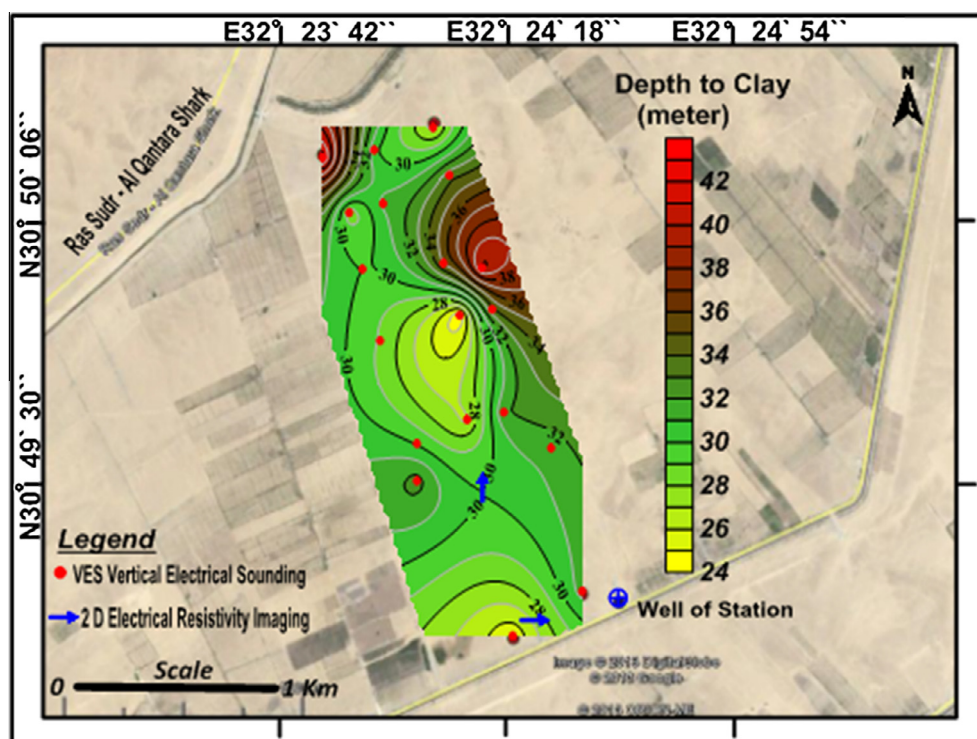


Figure 17 Depth to clay layer contour map.

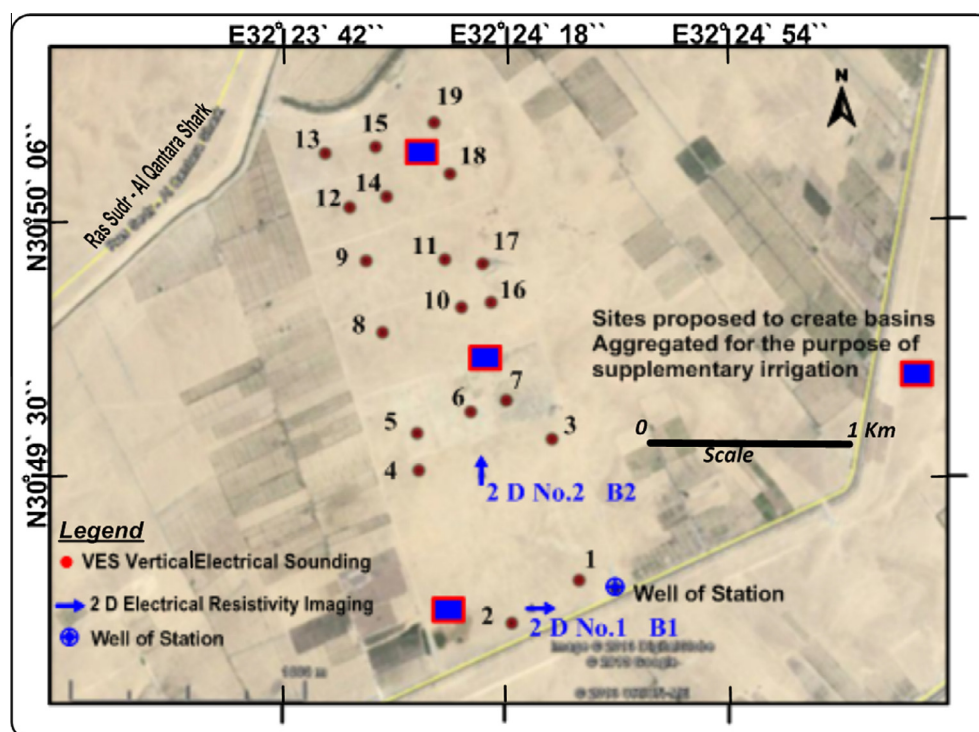


Figure 18 Location of sites proposed to create basins situated for the purpose of supplementary irrigation.

There is an analytical solution for safe yield of drilled wells. Calculation of safe yield needs to know the type of well, total depth of well and well design. Well design and safe yield can be calculated from the Ghyben-Herzberg relation (Todd, 1980) and discussed as follows:

1. Hand dug well: This type of well is recommended at areas lying near to ocean shores. These wells have 3 m in diameter ($2r$) and if, for example, thickness of water (Z) reaches 5 m (Fig. 19a), the safe yield (Q) of these wells can then be calculated by the following equation:

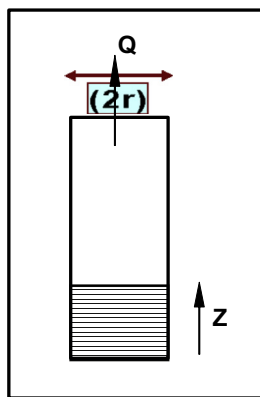


Figure 19a Hand dug well.

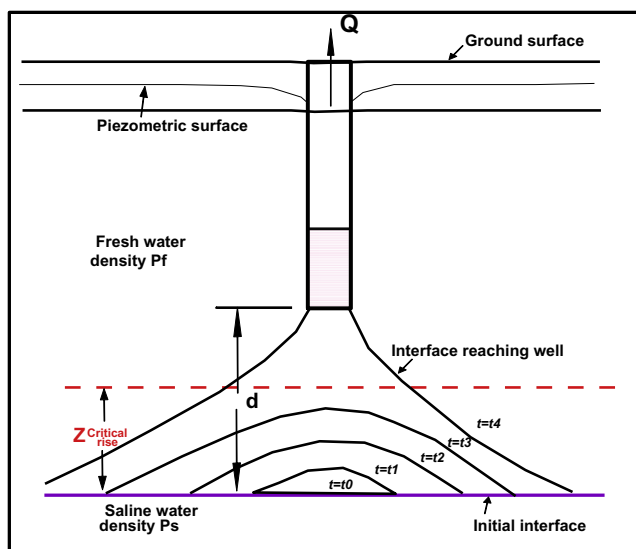


Figure 19b Drilled well.

$$Q = \pi r^2 Z m^3$$

where r is the half diameter of the well and Z is the thickness of water.

$$\text{Then, } Q = 3.14 \times (1.5)^2 \times 5 = 35.33 \text{ m}^3.$$

The discharge of the hand dug well would be two times per day, in the morning and in the evening. The total safe yield of each such hand dug well is (Q) $35.33 \text{ m}^3/\text{day}$.

2. Drilled well: This type of well (Fig. 19b) is recommended and can be dug where thickness of the brackish water exceeds 25 m and depth to the saline interface is more than 35 m. Due to the up-coning of the brackish-saline water interface during pumping, the safe yield (Q) for every well can be calculated according to the following equation:

$$Z = Q / [2\pi d^2 k(\Delta\rho/\rho_b)]$$

where $\Delta\rho = \rho_s - \rho_b$; ρ_s (1.025), ρ_b (1.0) is the specific weight of saline and brackish water.

K = Hydraulic conductivity. Z = the critical rise.

d = the distance between the end of the well and interface between saline and brackish water.

If the up-coning exceeds a certain critical rise (z), it accelerates upwards in the well (Fig. 19b). Critical rise (z) has been estimated to approximate $Z/d = 0.3-0.5$. Thus, adopting an upper limit of $Z/d = 0.5$ is recommended.

5. Conclusions and recommendation

The Sinai Peninsula has enormous development potential, especially in agricultural activities to supply growing settlements and communities. This development process increased the demand for water. The continuous availability of research services and scientific guidance becomes important for development. Thus, many research stations are constructed by the Desert Research Center covering desert land in Egypt. One of these stations is at South Qantara Shark that was constructed in northwestern Sinai for solving problems related to agriculture, and is also considered as a productive station. The present study concentrates on the area of this station having length reach to 1600 m. and width 850 m. The surface and subsurface layers belonging to Quaternary deposits consist of sand, sandy clay and clay facies of Pleistocene age. This station suffers from shortage of water supply for agriculture in some seasons, especially in summer, because it depends on a tributary of the El Salam canal that does not always contain water. There is one drilled well for human use just south of the study area with a total depth of 21 m and depth to water reaches 11 m. Its salinity has been recorded as 2528 ppm. Some patches of water logging appear in low land in the SW part of the area because of the inexistence of a good drainage system. Geoelectrical resistivity techniques were used in the present study to deal with previously mentioned conditions. The appropriate solutions to these problems have been delineated by the results of 1D and 2D geoelectrical measurements. They reveal the subsurface sedimentary sequences and extension of subsurface layers in the horizontal and vertical directions. Additionally, the resistivity assisted in choosing the most suitable places to drill or excavate production wells with good possibilities and quality.

Nineteen of Vertical Electrical Soundings (VESs) were arranged in a grid to cover the study area and two 2D geoelectrical imaging profiles were carried out. The results of geoelectrical interpretations indicated a number of layers that were grouped together in three main layers. The first layer is surface layer "A" and the second is layer "B" which was divided according to resistivity values into two zones (B1 and B2) that act as water bearing layers, while the last one is layer "C". The results are represented through different contour maps and cross sections that exhibit the horizontal distribution of successive layers which reflect the lithology and extent of change in all directions. The results mapped the thickness of the water bearing layers (B) which consisted of two zones. The upper one (B1) was less salty than the lower one (B2). The thickness of the upper zone ranged from 5 to 7 m but the lower zone ranged from 15 to 30 m. The last detected layer is clay that decreases in depth toward the southwest of the study area causing the phenomenon of water logging.

According to the results of geoelectrical measurements, the two saturated zones (B1 and B2) exhibited different salinity degrees. The upper saturated zone (B1) contains good quality groundwater and lower degree of salinity than the lower saturated zone (B2) according to resistivity values. So, it is recommended that the determination of the safe yield is necessary to

prevent mixing of the groundwater of both saturated zones (B1 and B2) during discharge from wells and consequence its harmful effect on cultivation. This phenomenon is known as up-coning, by over pumping. When this occurs, it generally necessitates that the well has to be shut down because of the influence of the saline water by a local rise of the interface between the saline and brackish water below the well.

The highest priority sites for drilling productive wells for supplementary irrigation in the study area are at the NW and SE directions. These wells must be drilled with a total depth not exceeding 30 m. The suitable technique for drilling is hand dug but it is possible to use rotary drilling to a depth less than the saline interface as revealed by the resistivity work. The drilled wells must be constructed with a suitable casing, with screen carefully placed at a certain distance above the saline interface. Also, pumping tests are important for determining safe yield and also may serve to locate high permeability areas with good quality of groundwater recharge. The discharge from hand dug well would be limited to two times per day, in the morning and in the evening. The total safe yield of every hand dug well is (Q) 35.33 m³/day when these wells have 3 m in diameter and thickness of water is at least 5 m.

It is recommended to construct three cement storage basins with dimensions of 3 * 20 * 20 m because of the small thickness of the upper saturated zone (B1), which is approximately 5 m of good quality groundwater. These basins permit collecting approximately 1200 m³ of water. The collected water can be used during shortage of water from the local tributary of the El Salam canal. The distribution of these basins should be in the SW and NE corners, and in the center of the study area.

The most suitable place for a drainage system is to construct it in the SW part of the area because of the dip and shallow depth of the clay layer. Reuse of the water of water logging must be done with caution and using the drip irrigation method or other advanced irrigation methods in the study area, not allowing flood irrigation method to avoid water logging preamble and prevent the salt marsh formations, where the clay layer is near the surface.

References

- Acworth, R.I., Dasey, G.R., 2003. Mapping of the hyporheic zone around a tidal creek using a combination of borehole logging, borehole electrical tomography and cross-creek electrical imaging. *Hydrogeol. J.* 11, 368–377.
- Basheer, A.L., Hussein A., Osman, Salah S., Tahal, Ayman I., 2012. Assessment of the Saline-Water Intrusion through the Fresh Groundwater Aquifer by Using ER and TEM Methods at the Qantara Shark Area, Sinai Peninsula, Egypt. *Int. J. Innov. Res. Develop.* 3 (4), 398–406.
- Ball, J., 1939. Contribution to the Geography of Egypt. Survey Dep. Egypt. Cairo, p. 300.
- Barseem, M.S., 2011. Delineating the conditions of groundwater occurrences in the area south Baloza – Romana road – North West Sinai – Egypt. *Egypt. Geophys. Soc. EGS J.* 9 (1), 135–143.
- Barseem, M.S., El Tamamy, Ayman M., Masoud, Milad H.Z., et al., 2013. Hydrogeophysical evaluation of water occurrences in El Negila area, Northwestern coastal zone – Egypt. *J. Appl. Sci. Res.* 9 (4), 3244–3262.
- Choudhury, K., Saha, D.K., Chakraborty, P., 2001. Geophysical study for saline water intrusion in a coastal alluvial terrain. *J. Appl. Geophys.* 46, 189–200.
- Deiab, A.F., 1998. Geology, pedology and hydrogeology of the Quaternary deposits in Sahl El Tinah area and its vicinities for future development of North Sinai, Egypt. Ph.D. Thesis, Geol. Dept., Fac. Sci., Mansoura Univ., Egypt, p. 242.
- El Austa, M.M., 2000. Hydrogeological study for Evaluation on the area between El Qantara and Ber El-Abd, North Sinai –Egypt. M. Sc. thesis Geol. Dep. Fac. of Sci. Minufiya Univ., p. 162.
- El Shamy, I.Z., 1983. On the Hydrology of West Central Sinai. *Egypt. J. Geol.* 27 (1–2), 2.
- El Waheidi, M.M., Merlanti, F., Paven, M., 1992. geoelectrical resistivity survey of the central part of Azraq Basin (Jordan) for identifying saltwater/freshwater interface. *J. Appl. Geophys.* 29, 125–133.
- Frohlich, R., 1974. Combined geoelectrical and drill-hole investigations for detecting freshwater aquifers in northwestern Missouri. *Geophysics* 39, 340–352.
- Geological Survey of Egypt (GSE), 1992. Geological map of Sinai, A. R.E. Sheet No. 5, Scale 1:250,000.
- Griffiths, D.H., Barker, R.D., 1993. Two-dimensional resistivity imaging and modeling in areas of complex geology. *J. Appl. Geophys.* 29, 211–226, Elsevier Science Publishers, B.V., Amsterdam.
- Khaled, M.A., Galal, G.H., 2012. Study of groundwater occurrence and the impact of salt water intrusion in East bitter lakes, Northwest Sinai, Egypt by using the geophysical techniques. *Egypt. Geophys. Soc. EGS J.* 10 (1), 1–12.
- Loke, M.H., 1998. RES2DINV". V.3.4, "Rapid 2-D resistivity inversion using the least-square method. ABEM instruments AB, Bromma, Sweden.
- Mares, S., 1984. Introduction to Applied Geophysics. D-Re- dial Pub. Com, Dordrecht.
- Orellana, E., Mooney, H.M., 1966. Master tables and curves for vertical electrical sounding over layered structures. Interciences, Madrid, 34.
- Ritz, M., Parisot, J.-C., Diouf, S., Beauvais, A., Dione, F., 1999. Electrical imaging of lateritic weathering mantles over granitic and metamorphic basement of eastern Senegal, West Africa. *J. Appl. Geophys.* 41, 335–344.
- Said, R., 1962. The geology of Egypt. Elsevier Pub. Co., Amsterdam.
- Shata, A., 1956. Structural development of the Sinai peninsula, Egypt. *Bull. Inst. Desert, Egypt* 6 (2), 117–157.
- Seaton, W.J., Burbey, T.J., 2000. Aquifer characterization in the Blue Ridge physiographic province using resistivity profiling and borehole geophysics. *J. Environ. Eng. Geophys.* 5 (3), 45–58.
- Todd, D.K., 1980. Groundwater Hydrology, 2nd edition. John Wiley & Sons, New York.
- Van Der Verpen, B.P.A., 1988. RESIST, version 1.0, a package for the processing of the resistivity sounding data. M.Sc. Research project. ITC, Delft, the Netherlands.
- Zohdy, A.A.R., 1989. A new method for automatic interpretation of Schlumberger and Wenner sounding curves. *Geophysics* 54, 244–253.